OPTIMAL TRANSPORT BASED CONTROL OF GRANULAR IMAGING SYSTEM IN SPACE

Saptarshi Bandyopadhyay*, **Marco B. Quadrelli**†

"Orbiting Rainbows" is a paradigm for creating a space-based observatory (telescope) from confined and aligned granular media. The overall objective is to construct a very large and lightweight aperture in space using a cloud of micron-sized particles held in position and aligned by the application of external electromagnetic fields, thus alleviating the extreme expense of deploying and stabilizing large monolithic telescopes by reducing the mass of the primary aperture. Adaptive optics techniques for wavefront stabilization and computational imaging techniques are then used to remove the optical noise from the scattering reflections of the granular medium, and finally producing clean images within the diffraction limit. In this paper, we address one of the key challenges of this new paradigm, namely controlling the position and orientation of the granules or particles so that the cloud of particles achieves the desired shape of an ultra-lightweight telescope and points into the right orientation. A further complication arises due to the fact that the particles do not have any onboard actuators. A number of external electric-field-based actuators are used to control all the particles simultaneously. Moreover, the number of actuators are orders-of-magnitude smaller than the number of particles, making this system largely under-actuated. Since the cloud of particles in any plausible configuration can be modeled as a probability distribution over the workspace, we formulate this control challenge as an optimal transport problem and then show that our optimal transport based control law drives the cloud of particles from any initial distribution to the desired position distribution (optical surface) and angular distribution (polarization state). Simulation results demonstrate the effectiveness of our approach.

INTRODUCTION

"Orbiting Rainbows" was initially developed under a Phase II NASA Innovative Advanced Concepts (NIAC) study, This study looked at twenty years into the future of creating a space-based observatory from confined and aligned granular media.[?, 1, 2] The goal of this research is to identify ways to optically manipulate and maintain the shape of a cloud of dust-like matter so that it can function as an adaptive surface with useful electromagnetic characteristics in the optical or microwave bands. The investigators have been performing fundamental research and developing the technology roadmap to construct an optical system in space using nonlinear optical properties of a cloud of micron-sized particles, shaped into a specific surface by light pressure, to form a very large and lightweight aperture of an optical system. This "cloud optic" would be relatively simple to package, transport, and deploy. It would be reconfigurable and could be re-targeted; the focal length would be variable and it would be self-healing and ultimately disposable. With near-term

*Robotics Technologist, Jet Propulsion Laboratory (JPL), California Institute of Technology (Caltech), Pasadena, California, 91109, USA; Saptarshi.Bandyopadhyay@jpl.nasa.gov
†Research Technologist and Group Lead, Robotics Controls, Decision, and Estimation Group, Jet Propulsion Laboratory, California Institute of Technology, Pasadena, California, 91109, USA; Marco.B.Quadrelli@jpl.nasa.gov

plans to build 30 meter ground-based telescopes for astronomy, the demand for higher resolution optics in space continues to grow not only for exo-planet detection, but also for earth-based science, including hyper-spectral imaging and for monitoring of the oceans and land masses (e.g. seismic monitoring). This concept, in which the aperture does not need to be continuous and monolithic, would increase the aperture size several times compared to large NASA space-borne observatories currently envisioned, allowing for a true Terrestrial Planet Imager that would be able to resolve exo-planet details and do meaningful spectroscopy on distant worlds, with orders of magnitude less total system cost and complexity.

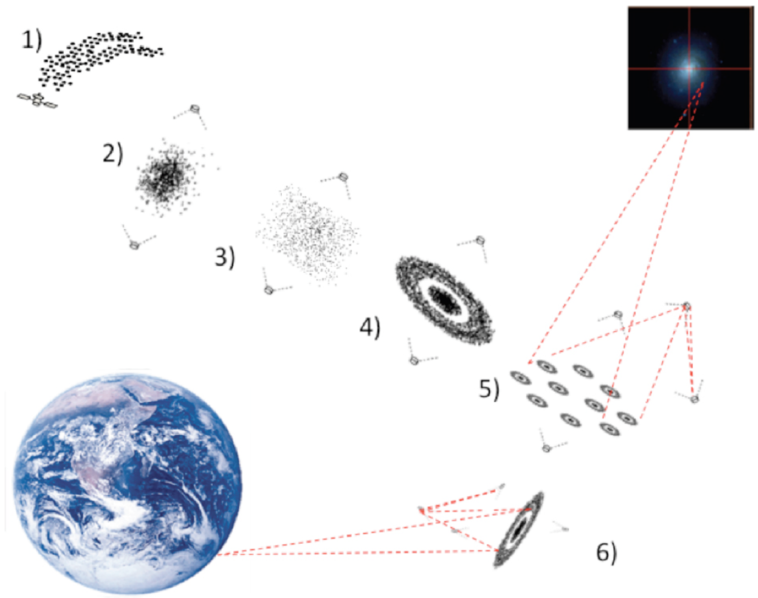

Figure 1. Sequence for Granular Telescope deployment and commissioning (Reproduced with permission from Ref. 1)

After considering refractive, reflective, and holographic systems and their associated optical correction and collection systems, an optical imaging system design was selected as the best candidate architecture for a space system involving a cloud of particles. As shown in Fig. 1, the sequence of optics would as follows: the starlight is focused by granular spacecraft optic path, creating a spherical wavefront. Light from all patches would converge at an intermediate focus, which has an image-plane coded aperture (or random mask). The light would then reflect off secondary mirror (Gregorian) and the light from each patch would then be collimated. Each beam would go to a separate adaptive optics system. A fast steering mirror and a deformable mirror would correct for optical beam pointing and low to mid-spatial frequency aberrations. An optical delay line would be used to correct phasing difference between the patches and allow for Fourier transform spectroscopy. A beam-splitter would also be included to allow some of the light to go to a Shack-Hartmann sensor in order to measure aberrations in the system. Imaging architectures in the radar band have also been considered, with the goal of focusing scattered energy to obtain higher resolution imaging or imaging in areas of the target body that would have been previously inaccessible. In this paper, we address one of the key challenges of this new paradigm, namely controlling the position and orientation of the granules or particles so that the cloud of particles achieves the desired shape of an ultra-lightweight telescope and points into the right orientation. A further complication arises due to the fact that the particles do not have any onboard actuators. A number of external electric-

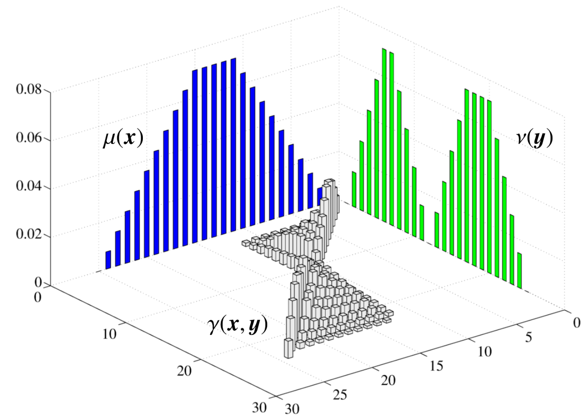

Figure 2. The initial probability mass function (pmf) $\mu(x)$ (in blue) is transported to the desired pmf $\nu(\boldsymbol{y})$ (in green) while minimizing the cost function $c(\boldsymbol{x}, \boldsymbol{y}) = \|\boldsymbol{x} - \boldsymbol{y}\|_2$. The optimum transference plan $\gamma(\boldsymbol{x}, \boldsymbol{y})$ is shown in gray. (Reproduced with permission from Ref. 3)

field-based actuators are used to control all the particles simultaneously. Moreover, the number of actuators are orders-of-magnitude smaller than the number of particles, making this system largely under-actuated. Since the cloud of particles in any plausible configuration can be modeled as a probability distribution over the workspace, we formulate this control challenge as an optimal transport problem and then show that our optimal transport based control law drives the cloud of particles from any initial distribution to the desired position distribution (optical surface) and angular distribution (polarization state). We show that our optimal transport based control law drives the cloud of particles from any initial distribution to the desired distribution and polarization so that it can function as an ultra-lightweight surface with useful and adaptable electromagnetic characteristics.

Optimal transport (OT) is an optimization approach that is used to find the optimum transference plan from an initial distribution to the desired distribution with respect to the given cost function.[4] An example of OT is shown in Fig. 2. OT has been previously used for the formation control of spacecraft swarms, where each spacecraft has its own independent actuator.[3]

Note that in our case, the number of actuators are orders-of-magnitude smaller than the number of particles. The question we address is then:

> Is it possible to arbitrarily shape and align the N grains of a granular medium with $n <<< N$ actuators placed outside the granular medium domain, i.e. with at-a-distance exogenous, non-contact, actions?

The results described in this paper confirm that it can be done.

This paper is organized as follows. The problem statement is presented in Section 2. The OT problem formulation and control law are presented in Section 3. Simulation results in Section 4 demonstrate the effectiveness of our approach. This paper is concluded in Section 5.

MODELING OF DIFFUSE MEDIUM

There are many techniques to model the dynamics of diffuse media, such as a cloud: Cellular Automata,[?] Lattice-Boltzmann Hydrodynamics,[?] to name a few. A description of the cloud dynamics within a spatial domain Ω can be cast as a boundary value problem as

$$[\Gamma(x,t) + \Sigma(x,t;\omega)]u(x,t;\omega) = f(x,t;\omega) + f_c(x,t) \tag{1}$$

together with the appropriate boundary conditions at the boundary of Ω, where x is the spatial scale, t is the temporal scale, ω is a random fluctuation, Γ is the deterministic operator describing the dynamics, Σ is the stochastic part of the dynamical operator whose coefficients are zero-mean random processes, u is the displacement of a grain of the cloud, f is the vector of exogenous disturbances, and f_c is the vector of control inputs. For a diffuse medium, two time scales enter the picture, as well as two spatial scales. The individual grain dynamics begins to emerge when $(\lambda/L)1$, where λ is the time (or space) scale of the stimuli internal or external to the cloud, whereas L is a time (or space) scale representative of the cloud itself. When $(\lambda/L) << 1$, the individual grain behavior is predominant, and when $(\lambda/L) >> 1$, the cloud behavior as a unit is predominant, therefore it could be considered as an effective rigidified medium (rigid body). In this paper, to keep the problem tractable, we limit our analysis to a two-dimensional problem with N=1000 particles (rigid bodies). Furthermore, we consider that the dynamics equations have already been discretized in time and space, leading to a set of algebraic equations. For instance, and denoting the particle displacement by p_k^ℓ, and using an Euler step, the point mass displacement dynamics of a unit mass particle can be expressed as

$$p_{k+1}^\ell = p_k^\ell + \Delta f_c \,. \tag{2}$$

where Δ is the time step size. This is analogous to assuming that the dynamics follows the equation of a double integrator in frequency space, and an adequate modeling assumption for purposes of this study.[?]

GRANULAR IMAGER CONTROL APPROACH

A granular imager is a space-borne imaging system that makes use of a collection of small reflective grains to form a sparsely filled primary mirror or aperture. Light reflected from each grain is then focused into a back-end system consisting of a control system and detector. However, to be an effective imager with a useful point spread function (PSF), the wavefronts reflected from the parabolic surface of the cloud must be corrected. A control system must be used in conjunction

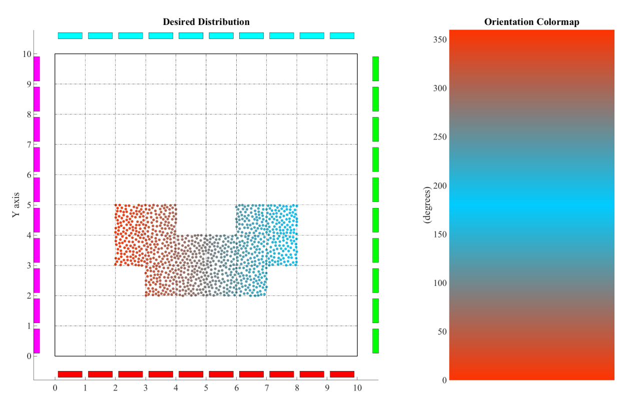

Figure 3. The desired distribution and orientation of $N = 1000$ particles are shown. The 40 actuators on the boundary of the workspace and orientation colormap are also shown.

with the external confinement and alignment system to correct the wave-fronts so that the granular imager will generate high resolution image that fully realize the potential of larger aperture sizes. The challenge of a wavefront control system for a granular imager is to correct for the scattered speckle field when the effective surface roughness of the granular media is on the order of microns. It is unlikely that a single deformable optic will have both the range and control accuracy to correct for such roughness. Therefore, a multi-stage control architecture is needed.

The wavefront control process follows the following steps. First, the Granular Cloud Shaping step, in which grains are trapped in an optical or ion trap, where they are shaped into the surface of a parabola. Second, the Sub Aperture Coarse Alignment step, in which the trapped grains may be broken into regions or sub-apertures for easier management. Correcting for coarse misalignments between sub-apertures, corrects the low spatial frequency surface roughness of our granular imager, thereby making the point spread function of the granular imager more compact. Third, the Figure Control step: now that each sub-aperture is controlled globally with respect to each other, the figure of each sub-aperture can be controlled. Fourth, the Computational Imaging step, in which a combination of PSF deconvolution techniques and computational imaging will be used to compensate for less-than-ideal imaging as a result of the granular nature of the primary mirror. Mode details can be found in the NIAC Phase II Final Report.

This paper specifically addresses the first and second step of the diffuse medium shaping and alignment control. The specific electrodynamic trapping control mechanisms are discussed in another paper.[?]

PROBLEM STATEMENT

Assume a cloud of $N \in \mathbb{R}$ particles in 2D space.[*]

Our objective is to start from any distribution and achieve the desired positions and orientations shown in Fig. 3. The boundary of the workspace has 4 set of 10 actuators. All the $N = 1000$ particles are controlled using only these 40 actuators. Note that the workspace is partitioned into a 10×10 grid due to the actuators. We shall call these 100 squares as bins.

We now describe the position and orientation dynamics of the particles. Let $p_k^\ell \in \mathbb{R}^2$ represent the position of the ℓ^{th} particle at the k^{th} time instant, where $\ell \in \{1, \ldots, N\}$. Moreover, let the ℓ^{th} particle lie in the bin $[i, j]$, as shown in Fig. 4. All the particles in the bin $[i, j]$ experience the forces from the actuators $a_{1,i}$ (red), $a_{2,j}$ (green), $a_{3,i}$ (cyan), and $a_{4,i}$ (magenta) and the strength of the forces varies inversely with the distance from the actuators. Therefore, the ℓ^{th} particle's position dynamics is given by

$$\begin{aligned} p_{k+1}^\ell = & p_k^\ell + \Delta \left(\frac{a_{1,i}}{dis(\ell, a_{1,i})}\hat{y} - \frac{a_{2,j}}{dis(\ell, a_{2,j})}\hat{x} - \frac{a_{3,i}}{dis(\ell, a_{3,i})}\hat{y} + \frac{a_{4,j}}{dis(\ell, a_{4,j})}\hat{x} \right) \\ & + \Delta \sum_{m \in N, m \neq \ell} a_{rep} \frac{p_k^\ell - p_k^m}{\|p_k^\ell - p_k^m\|_2^3} , \end{aligned} \tag{3}$$

where Δ is the time step size, $\hat{x}$ and $\hat{y}$ are the unit vectors along X and Y axis, and $dis(\ell, a_{1,i})$ represents the distance between the ℓ^{th} particle and the $a_{1,i}$ actuator. In addition, the ℓ^{th} particle also experiences a very small repulsion from its neighboring particles that varies inversely as the square of the distance between them.

[*]The extension of our concepts to a 3D workspace is straight-forward but outside the scope of this paper.

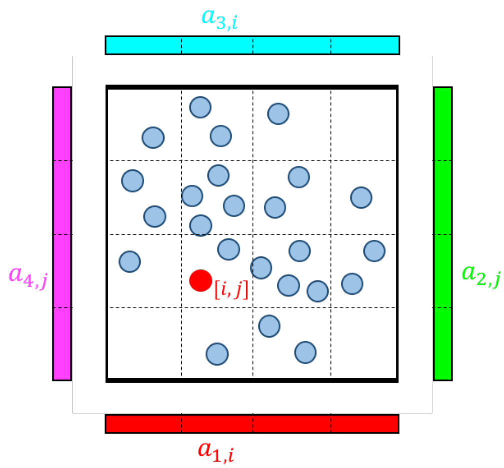

Figure 4. The red particle in the bin $[i, j]$ experiences the forces from the actuators $a_{1,i}$ (red), $a_{2,j}$ (green), $a_{3,i}$ (cyan), and $a_{4,i}$ (magenta).

Similarly, let $\theta_k^\ell \in SO(2)$ represent the orientation of the ℓ^{th} particle at the k^{th} time instant. The actuators $a_{1,i}$ (red) and $a_{3,i}$ (cyan) in Fig. 4 together setup a common orientation angle θ_i for all particles in bin $[i, j]$. Therefore, the ℓ^{th} particle's orientation dynamics is given by

$$\theta_{k+1}^\ell = (1 - \Delta)\theta_k^\ell + \Delta\theta_i \,. \tag{4}$$

Thus the objective of this paper is to derive a control law that specifies actuator strengths $a_{1,i}$, $a_{2,j}$, $a_{3,i}$, $a_{4,j}$, $\forall i, j \in \{1, \ldots, 10\}$, and desired orientations $\theta_i, \forall i \in \{1, \ldots, 10\}$ during each time instant so that the cloud of N particles achieve the the desired positions and orientations shown in Fig. 3. We find such a closed-loop control law using optimal transport in the next section.

OPTIMAL TRANSPORT PROBLEM FORMULATION AND CONTROL LAW

Since the number of actuators is orders-of-magnitude smaller than the number of particles, common techniques used in the multi-agent control literature are not suitable for this application. Therefore, we transform the distribution of the cloud of particles into a probability distribution so that we can use the technique of optimal transport for this problem. For example, the cloud of particles shown in Fig. 4 can be transformed into a probability distribution as shown in Fig. 5.

Similarly, the desired distribution in Fig. 3 can also be transformed into a probability distribution as shown in Fig. 6. Let us denote this desired probability distribution with $\nu \in \mathbb{R}^{10\times10}$, where $\sum_{i=1}^{10}\sum_{j=1}^{10} \nu[i, j] = 1$.

Let the probability distribution of the cloud of particles at the k^{th} time instant be denoted by $\mu_k \in \mathbb{R}^{10\times10}$, where $\sum_{i=1}^{10}\sum_{j=1}^{10} \mu_k[i, j] = 1$. Therefore, the objective of this paper is to find a control law such that the probability distribution of the cloud of particles μ_k converges to the desired probability distribution ν.

Let l_{bin} represent the length or width of each bin. It follows from (3) that the force from actuator $a_{1,i}$ that would move all the particles in bin $[i, j]$ to the bin $[i, j + 1]$ is given by

$$a_{1,i,j,max} = \frac{1}{\Delta} l_{bin} dis(a_{1,i}, [i, j]) \,, \tag{5}$$

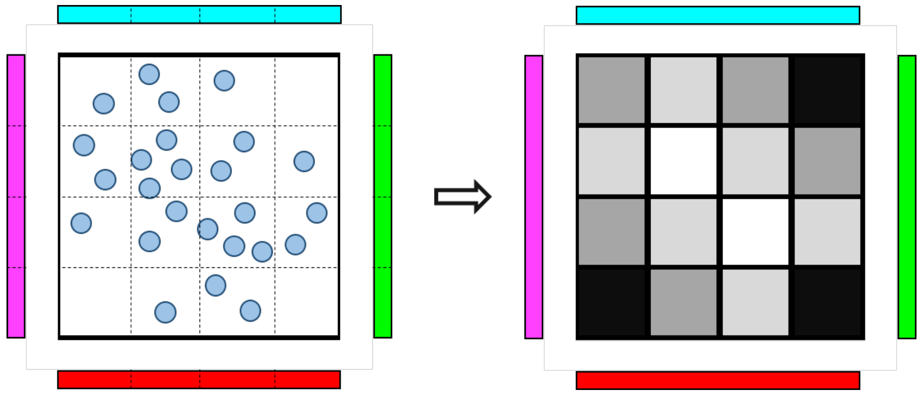

Figure 5. The cloud of particles shown in Fig. 4 is transformed into a probability distribution. The lighter bins contain more probability mass.

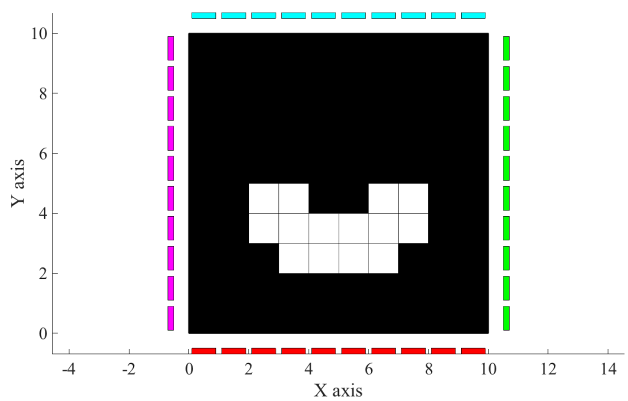

Figure 6. The desired probability distribution is denoted by ν.

where $dis(a_{1,i}, [i,j])$ represents the minimum distance from actuator $a_{1,i}$ to the bin $[i,j]$. If $a_{1,i} \leq a_{1,i,max}$, then we assume that the fraction of particles that be moved to the bin $[i, j+1]$ by this force is given by $\frac{a_{1,i}}{a_{1,i,j,max}}$. This is equivalent to stating that the probability of transitions from bin $[i,j]$ to bin $[i, j+1]$ due to actuator $a_{1,i}$ is given by $\frac{a_{1,i}}{a_{1,i,j,max}}$. We use this key insight for setting up the following optimal transport based convex problem to calculate the actuator strengths.

Optimal Transport based Convex Optimization Problem

$$\min_{\mu_{k+1},\, a_{1,i},\, a_{2,j},\, a_{3,i},\, a_{4,j}} D_{\mathcal{L}_2}(\mu_{k+1}, \nu) \tag{6}$$

subject to

$$\mu_{k+1}[i,j] \geq 0, \qquad \forall i,j \in \{1,\ldots,10\} \tag{7}$$

$$\begin{aligned}\mu_{k+1}[i,j] =& \mu_k[i,j]\left(1 - \frac{a_{1,i}}{a_{1,i,j,max}} - \frac{a_{2,j}}{a_{2,i,j,max}} - \frac{a_{3,i}}{a_{3,i,j,max}} - \frac{a_{4,j}}{a_{4,i,j,max}}\right)\\ &+ \frac{\mu_k[i,j-1]\,a_{1,i}}{a_{1,i,j-1,max}} + \frac{\mu_k[i+1,j]\,a_{2,j}}{a_{2,i+1,j,max}} + \frac{\mu_k[i,j+1]\,a_{3,i}}{a_{3,i,j+1,max}} + \frac{\mu_k[i-1,j]\,a_{4,j}}{a_{4,i-1,j,max}},\\ &\forall i,j \in \{1,\ldots,10\}\end{aligned} \tag{8}$$

$$0 \leq a_{1,i} \leq a_{1,i,1,max}, \qquad \forall i \in \{1,\ldots,10\} \tag{9}$$

$$0 \leq a_{2,j} \leq a_{2,10,j,max}, \qquad \forall j \in \{1,\ldots,10\} \tag{10}$$

$$0 \leq a_{3,i} \leq a_{3,i,10,max}, \qquad \forall i \in \{1,\ldots,10\} \tag{11}$$

$$0 \leq a_{4,j} \leq a_{4,1,j,max}, \qquad \forall j \in \{1,\ldots,10\} \tag{12}$$

Here $D_{\mathcal{L}_2}(\mu_{k+1}, \nu)$ represents the $\mathcal{L}_2$ distance between the probability distributions μ_{k+1} and ν. The transition probabilities are captured in (8). The terms $-\mu_k[i,j](\frac{a_{1,i}}{a_{1,i,j,max}} + \frac{a_{2,j}}{a_{2,i,j,max}} + \frac{a_{3,i}}{a_{3,i,j,max}} + \frac{a_{4,j}}{a_{4,i,j,max}})$ represent the probability mass flowing out of bin $[i,j]$ to neighboring bins. Similarly, the terms $+\frac{\mu_k[i,j-1]\,a_{1,i}}{a_{1,i,j-1,max}} + \frac{\mu_k[i+1,j]\,a_{2,j}}{a_{2,i+1,j,max}} + \frac{\mu_k[i,j+1]\,a_{3,i}}{a_{3,i,j+1,max}} + \frac{\mu_k[i-1,j]\,a_{4,j}}{a_{4,i-1,j,max}}$ represent the probability mass flowing into bin $[i,j]$ from neighboring bins.

Note that the constraint $\sum_{i=1}^{10}\sum_{j=1}^{10}\mu_{k+1}[i,j] = 1$ is not explicitly stated in the above optimization problem because it is implicitly satisfied by the conservation property of (8), i.e., $\sum_{i=1}^{10}\sum_{j=1}^{10}\mu_{k+1}[i,j] = \sum_{i=1}^{10}\sum_{j=1}^{10}\mu_k[i,j]$. Thus the above optimization problem is used to find the actuator strengths $a_{1,i}$, $a_{2,j}$, $a_{3,i}$, $a_{4,j}$, $\forall i,j \in \{1,\ldots,10\}$ based on the current probability distribution of the cloud of particles μ_k.

The control law for the desired orientations $\theta_i, \forall i \in \{1,\ldots,10\}$ is straight-forward, i.e., θ_i for each bin is set equal to that of the desired orientation in Fig. 3. The effectiveness of the orientation control laws is shown in Fig. 7.

NUMERICAL SIMULATIONS

The cloud of particles initially starts from a random distribution and orientation, as shown in Fig. 9(a). We show that this cloud of particles achieves the desired distribution and orientation in Fig. 3 using the control laws described in the previous section. The evolution of the cloud of particles over many time instants is shown in Fig. 9.

The $\mathcal{L}_1$ distance (convergence error) between the probability distributions μ_k and ν is shown in Fig. 8. This shows that the cloud of particles has achieved satisfactory convergence to the desired distribution after 100 time instants.

CONCLUSIONS

In this paper, we addressed one of the key challenges of the new Orbiting Rainbows paradigm. The Orbiting Rainbows paradigm synthesizes a space-based observatory (telescope) from confined

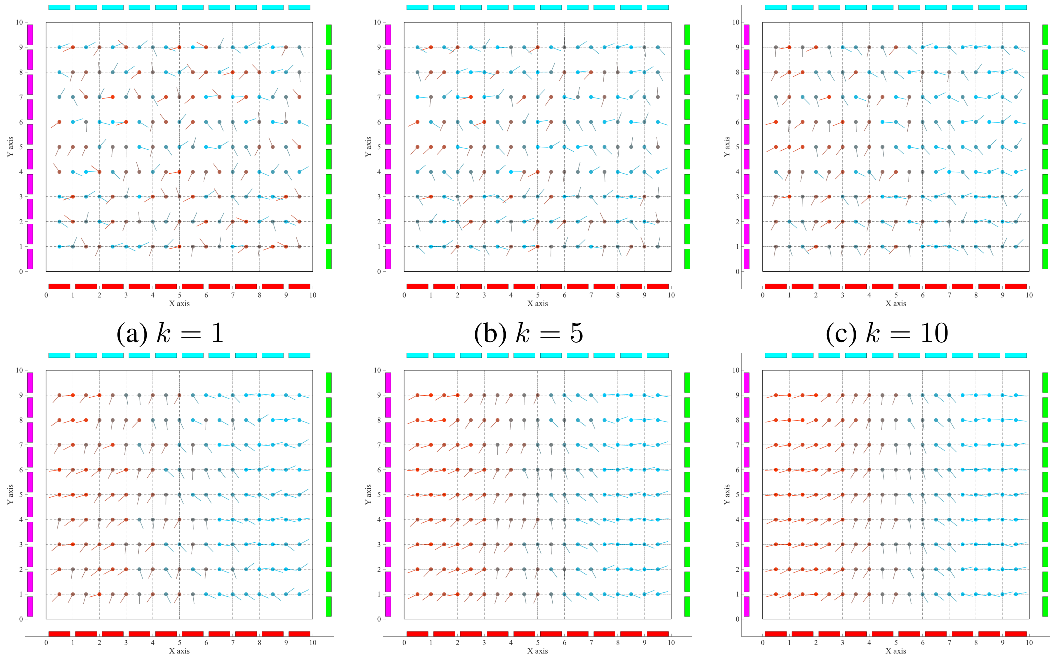

(a) $k = 1$ (b) $k = 5$ (c) $k = 10$

(d) $k = 15$ (e) $k = 20$ (f) $k = 25$

Figure 7. The evolution of the orientation of the cloud of particles is shown. Only the orientation control law is used here.

and aligned granular media. The overall objective is to construct a very large and lightweight aperture in space using a cloud of micron-sized particles held in position and aligned by the application of external electromagnetic fields, thus alleviating the extreme expense of deploying and stabilizing large monolithic telescopes by reducing the mass of the primary aperture. Adaptive optics techniques for wavefront stabilization and computational imaging techniques are then used to remove the optical noise from the scattering reflections of the granular medium, and finally producing clean images within the diffraction limit. Specifically, we addressed the challenge of controlling the position and orientation of the granules or particles of a diffuse medium so that a cloud of particles achieves the desired shape of an ultra-lightweight telescope and aligns the grains to the wavefront so a reflection can be obtained. A further complication arises due to the fact that the particles do not carry their own onboard actuators. A number of external electric-field-based actuators are instead used to control all the particles simultaneously. Moreover, the number of actuators are orders-of-magnitude smaller than the number of particles, making this system largely under-actuated. Since the cloud of particles in any plausible configuration can be modeled as a probability distribution over the workspace, we formulate this control challenge as an optimal transport problem and then show that our optimal transport based control law successfully drives the cloud of particles from any initial distribution to the desired position distribution (optical surface) and angular distribution (polarization state).

ACKNOWLEDGMENT

This research was funded by the NASA Innovative Advanced Concepts (NIAC) program under contract 14-14NIAC-II-0008 (Orbiting Rainbows, Phase II). This research was carried out at the Jet Propulsion Laboratory, California Institute of Technology, under a contract with the National

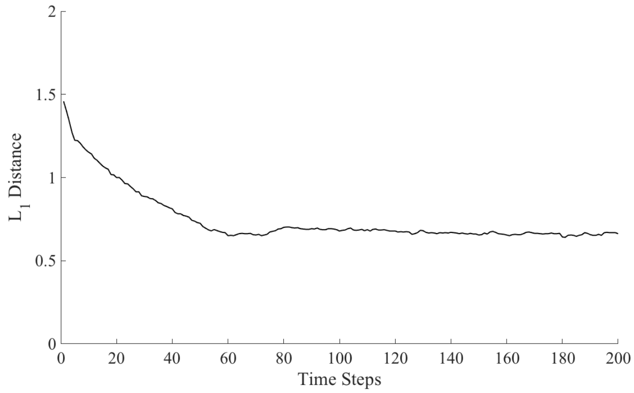

Figure 8. The convergence error with respect to time steps.

Aeronautics and Space Administration. Government sponsorship acknowledged.

REFERENCES

[1] M. B. Quadrelli, S. Basinger, G. Swartzlander, and D. Arumugam, "Dynamics and Control Of Granular Imaging Systems," *AIAA SPACE Conference and Exposition*, Pasadena, CA, 2015.

[2] S. A. Basinger, D. Palacios, M. B. Quadrelli, and G. A. Swartzlander, "Optics of a Granular Imaging System (i.e. "Orbiting Rainbows")," *SPIE Photonics Conference*, San Diego, CA, 2015.

[3] S. Bandyopadhyay, S.-J. Chung, and F. Y. Hadaegh, "Probabilistic Swarm Guidance using Optimal Transport," *Proc. IEEE Conf. Control Applicat.*, Antibes, France, Oct. 2014, pp. 498–505.

[4] C. Villani, *Optimal transport: Old and New*. Springer Verlag, 2008.

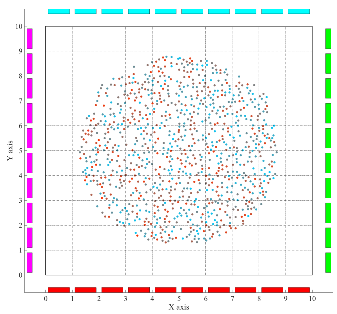

(a) $k = 1$

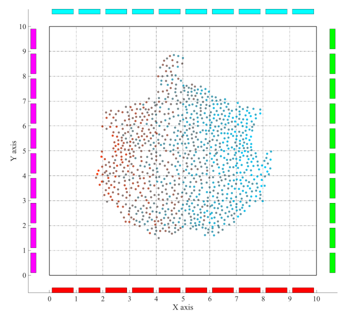

(b) $k = 10$

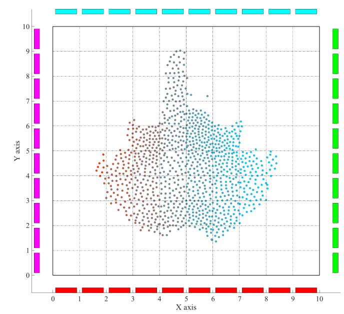

(c) $k = 20$

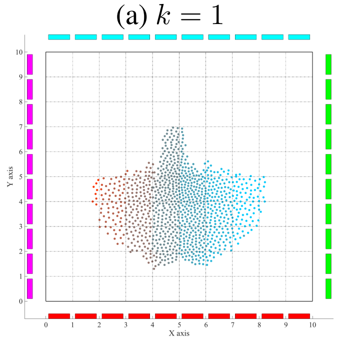

(d) $k = 40$

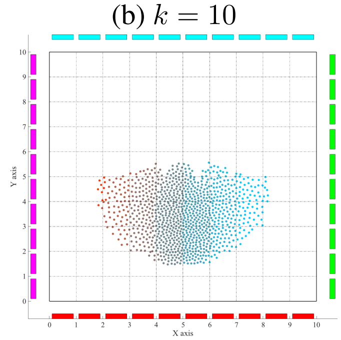

(e) $k = 60$

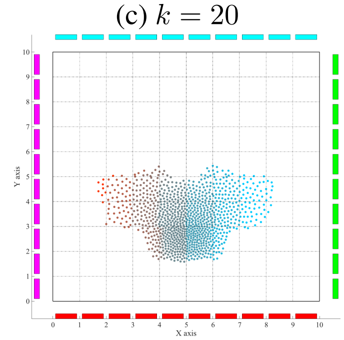

(f) $k = 80$

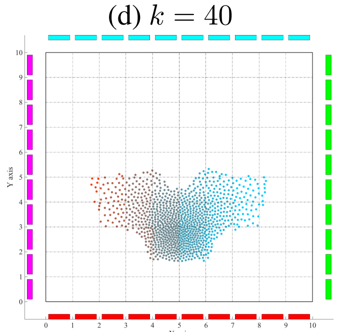

(g) $k = 100$

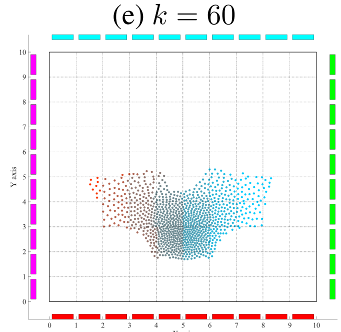

(h) $k = 150$

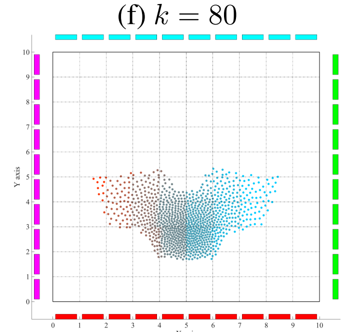

(i) $k = 200$

Figure 9. The evolution of the position and orientation of the cloud of particles is shown.